Magnetorotational Mechanism of Supernovae Explosion

G.S.Bisnovatyi-Kogan,
S.G.Moiseenko,
Space Research Institute, Moscow
N.V.Ardeljan, Moscow State University

KITP, 20 May, 2005

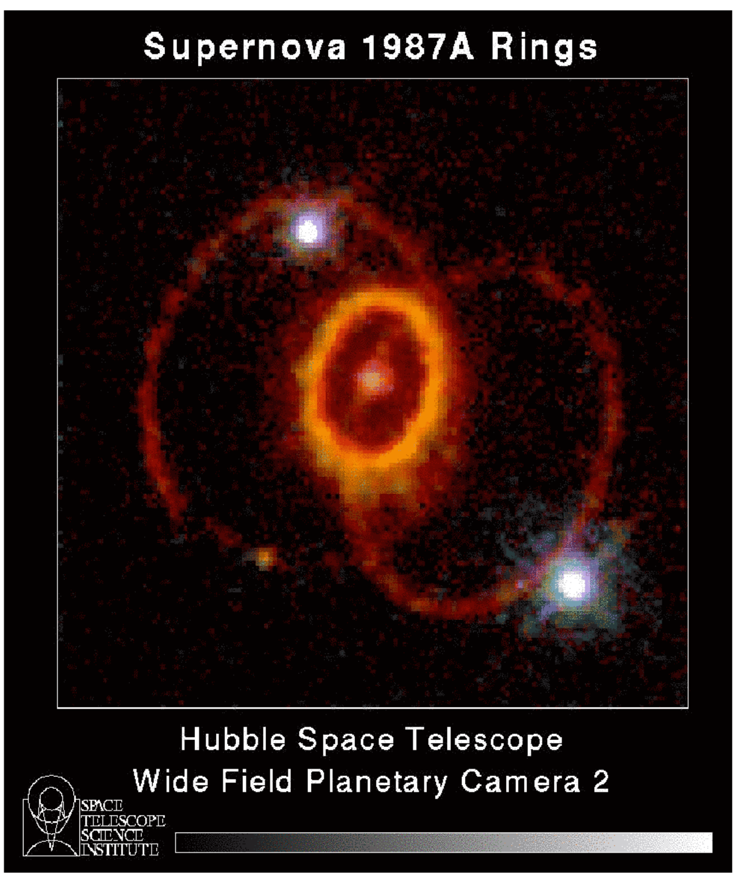

KITP, 20 May, 2005

Content

Presupernovae

- Magnetorotational mechanism of explosion
- 1-D calculations
- 2-D MHD: Numerical method.
- Core collapse and formation of rapidly rotating neutron star.
- Magnetorotational supernova explosion
- Development of magnetorotational instability
- Jet formation in magnetorotational SN explosion
- Mirror symmetry breaking: Rapidly moving pulsars. One-side jets.

Supernova is one of the most powerful explosion in the Universe, energy (radiation and kinetic) about 10^51 egr

End of the evolution of massive stars, with initial mass more than 8 Solar mass.

Explosion mechanism.

1. **Thermonuclear explosion** of C-O degenerate core **(SN Ia)**
2. **Core collapse and formation of a neutron star**, gravitational energy release 6 10^{53} erg, carried away by neutrino **(SN II, SN Ib,c)**

Transformation of the neutrino energy into kinetic one - ???

Magnetorotational explosion (MRE): transformation of the rotational energy of the neutron star into explosion energy by means of the magnetic field in core collapse SN

Hertzsprung-Russell diagram of the zero age main sequence.

Pols et al. (1995)

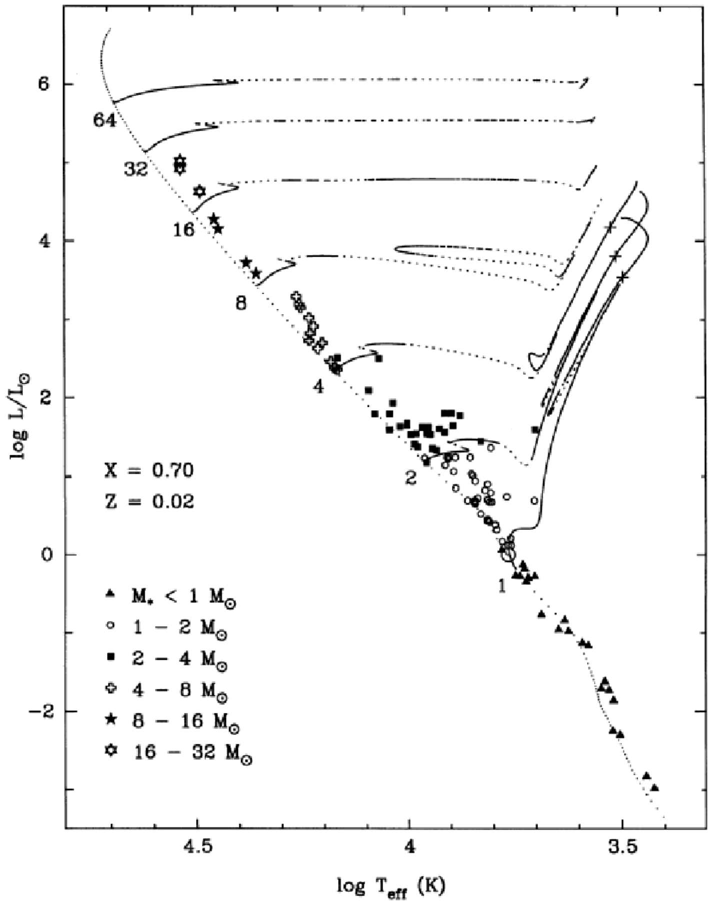

Log T_eff (K)

Figure 4. Hertzsprung–Russell diagram of the ZAMS and several evolutionary tracks, calculated with the updated stellar evolution code. The masses of the models are indicated at the starts of the tracks, in solar units. The solid portions of the tracks indicate where evolution is on a relatively slow nuclear time-scale, the dotted parts show evolution on a thermal time-scale, and the dashed parts show an intermediate time-scale. The

Tracks in HR diagram of a representative selection of stars from the main sequence till the end of the evolution.

Iben (1985)

enough to cause the previously ejected nebular matter to fluoresce. The result is known as a planetary nebula.

A summary of the evolutionary history of intermediate mass stars up to the point of planetary nebula excitation is given in Fig. 15 and in the caption for this figure.

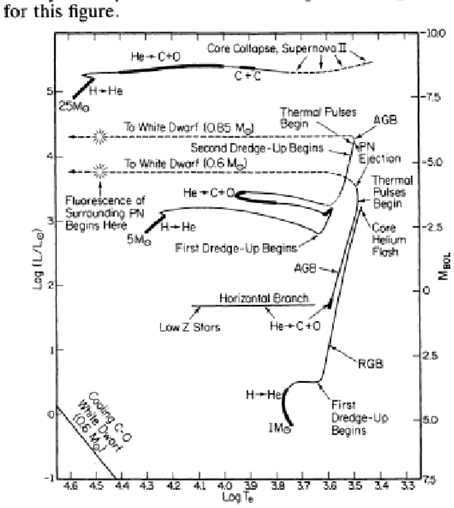

FIG. 15. Tracks in the HR diagram of a representative selection of stars. The heavy portions of each curve define locations where the major core nuclear burning phases occur. Details of tracks during transitory phases between major nuclear burning phases are suppressed. For stars of initial mass less than about 2·3 $M_\odot$, where in the HR diagram quiescent core helium burning (He → C+O) takes place after the core helium flash depends on the metallicity and on the extent of mass loss during the first red giant branch (RGB) phase. All stars which experience a core helium flash spend roughly 10^7 yr evolving upward along the 'early' asymptotic giant branch (E-AGB) burning helium in a shell. When helium is exhausted over about 0·53 $M_\odot$, hydrogen burning is rekindled and thermal pulses begin. How far a star evolves upward during the thermally pulsing AGB phase depends on the total mass of the star at the beginning of this phase, on the rate of mass loss by an ordinary stellar wind, and on the core-mass dependent critical mass in the hydrogen-rich envelope when planetary nebula (PN) ejection occurs. This latter phenomenon produces an expanding shell of matter and a remnant which evolves rapidly to the blue in the HR diagram, burning hydrogen at the base of a surface layer of very small mass. For a star of initial mass less than about 2 $M_\odot$, the lifetime in the TP-AGB phase is roughly 2×10^6 yr, the mass of a typical remnant is 0·6 $M_\odot$, and the time-scale for evolving to the blue far enough that photons from the surface

Most of supernova explosions and ejections are not spherically symmetrical. A lot of stars are rotating and have magnetic fields. Often we can see one-side ejections.

One of the main difficulties for supernova explosions how to transform any kind of energy of the star to the explosion energy.

Magnetorotational mechanism: transforms rotational energy of the star to the explosion energy.

In the case of the differential rotation the rotational energy can be transformed to the explosion energy by magnetic fields.

Bisnovatyi-Kogan, (1970) Astron. Zh.,**47**,813.

KITP, 20 May, 2005

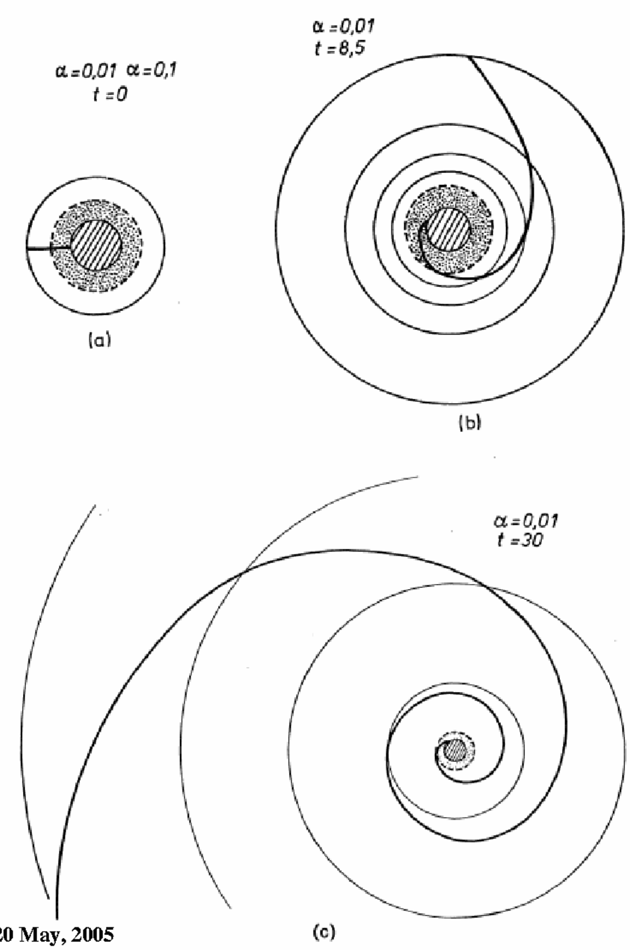

alpha=0.01,
t=8.5

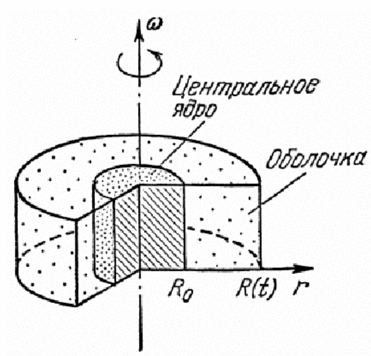

1-D calculations of magnetorotational explosion

B.-K., Popov, Samokhin (1976), Astrophys. Space Sci.,**41**, 321.

$$\alpha = \frac{E_{mag0}}{E_{grav}}.$$

KITP, 20 May, 2005

Fig. 5(a), (b), and (c) The configuration of the magnetic field line in the subsequent moments of

1-D calculations of magnetorotational explosion
B.-K., Popov, Samokhin (1976).

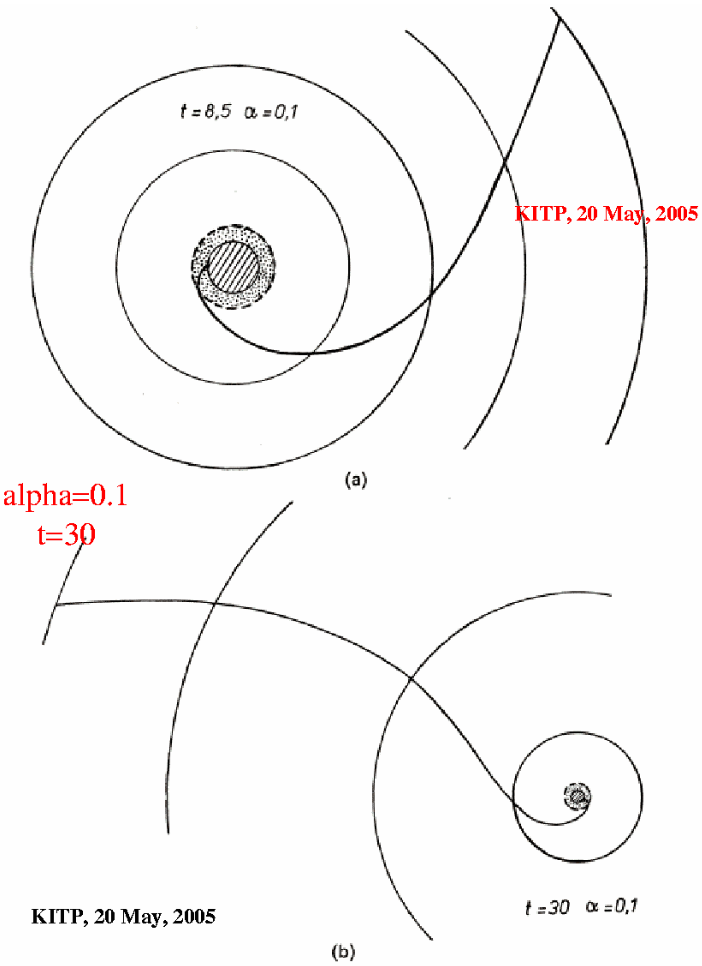

KITP, 20 May, 2005

Ardeljan, Bisnovatyi-Kogan, Popov (1979), Astron. Zh., **56**, 1244

$\alpha=10^{-2}$, 10^{-4}, 10^{-8}

$\alpha=10^{-2}$- dashed line, $\alpha=10^{-4}$- full line

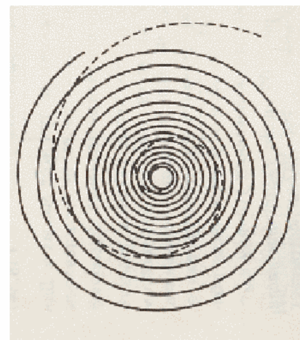

Angular velocity distribution at different time moments.

1-D calculations

B.-K., Popov, Samokhin (1976)

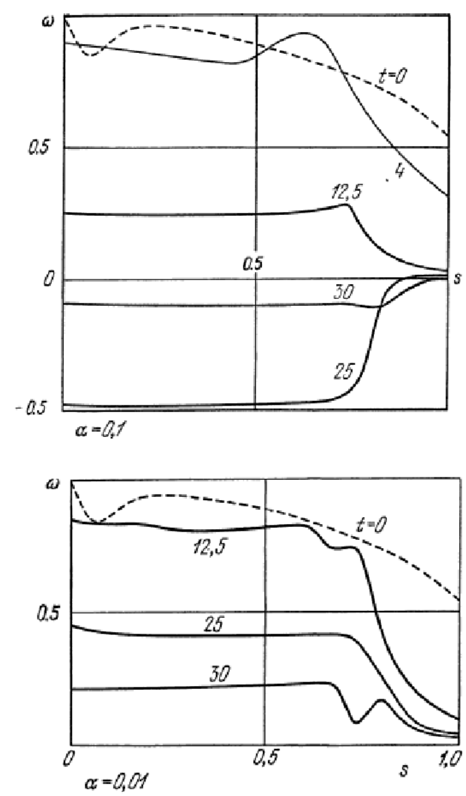

Fig. 3(a) and (b). The dependence of the angular velocity ω on the mass coordinate s at later time

KITP, 20 May, 2005

Variations of different types of energy during magnetorotational explosion.

1-D calculations

B.-K., Popov, Samokhin (1976)

THE MAGNETOHYDRODYNAMIC ROTATIONAL MODEL OF SUPERNOVA EXPLOSION 305

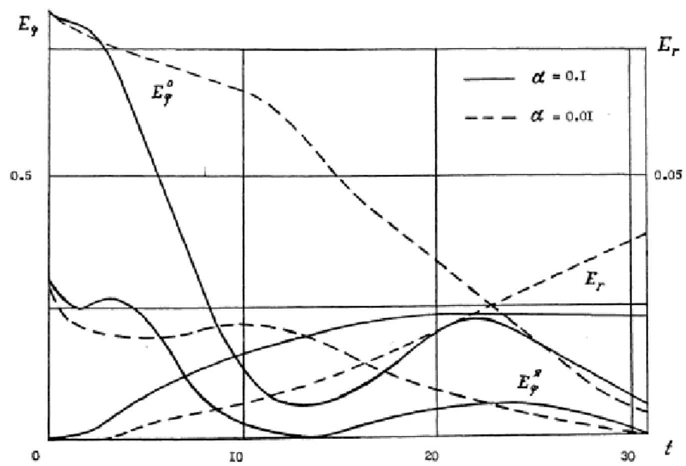

Fig. 7. The dependence of the kinetic energy on the time for two values of α: the rotational energy of the core E_φ^π, envelope E_φ^0, radial energy of the envelope E_r.

functions $E_\varphi^\pi(t)$ and E_φ^0 oscillate in time for $\alpha = 0.1$ with a monotonic increase of $E_r(t)$ reaching approximately constant value at $t = 30$. All these functions are monotonic in the case $\alpha = 0.01$; the energy of radial motion at the time $t = 31$ is 1.5 times larger in this case, than in the case of $\alpha = 0.1$ at the time $t = 30$.

The change of the rotational momentum J and angular velocity ω is represented on Figure 8 for the last mass point of the computer grid. The rotational momentum increases linearly in time for the late stages and the angular velocity decrease. Such a

The main results of 1-D calculations:

Magneto-rotational explosion (MRE) has an efficiency about 10% of rotational energy.

For the neutron star mass the ejected mass $\approx 0.1 M_\odot$,
Explosion energy $\approx 10^{51}$ erg
Ejected mass and explosion energy depend very weekly on the parameter α
Explosion time strongly depends on α .

$$\text{Explosion time} = \boxed{t_{\text{взрыва}} \sim \frac{1}{\sqrt{\alpha}}}$$

Small α is difficult for numerical calculations with EXPLICIT numerical schemes because of the Courant restriction on the time step, “hard” system of equations: α determines a “hardness”.

In 2-D numerical IMPLICIT schemes should be used.

First 2-D calculations.

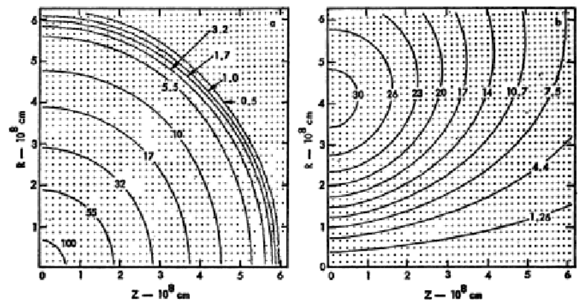

FIG. A1a.—Isodensity contours in units of 10^6 g cm^{-3} at 0.72 sec.
FIG. A1b.—Magnetic-flux contours parallel to Z-axis in units of 10^{12} gauss cm^{-2} at 0.72 sec.

Jets from collapse of rotating magnetized star: **density and magnetic flux**

LeBlanc and Wilson (1970)

Astrophys. J. **161**, 541.

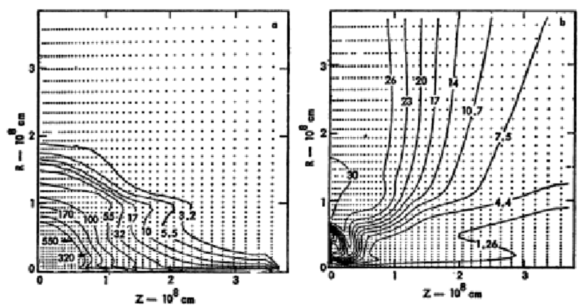

FIG. A2a.—Isodensity contours in units of 10^6 g cm^{-3} at 2.67 sec.
FIG. A2b.—Magnetic-flux contours parallel to Z-axis in units of 10^{22} gauss cm^{-2} at 2.67 sec.

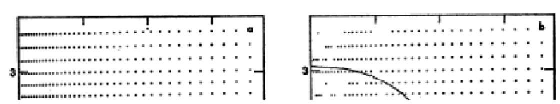

KITP, 20 May, 2005

Difference scheme (Ardeljan, Chernigovskii, Kosmachevskii, Moiseenko)

Lagrangian, on triangular grid

The scheme is based on the method of basic operators - grid analogs of the main differential operators:

GRAD(scalar) (differential) ~ GRAD(scalar) (grid analog)
DIV(vector) (differential) ~ DIV(vector) (grid analog)
CURL(vector) (differential) ~ CURL(vector) (grid analog)
GRAD(vector) (differential) ~ GRAD(vector) (grid analog)
DIV(tensor) (differential) ~ DIV(tensor) (grid analog)

The scheme is implicit.

It is developed and its stability and convergence are investigated by the group of N.V.Ardeljan (Moscow State University)

The scheme is fully conservative:

conservation of the mass, momentum and total energy,
correct calculation of the transitions between different types of energies.
Matrices for the transformation are symmetrical.

KITP, 20 May, 2005

Difference scheme: Lagrangian, triangular grid with grid reconstruction (completely conservative=>angular momentum conserves automatically)

Grid reconstruction

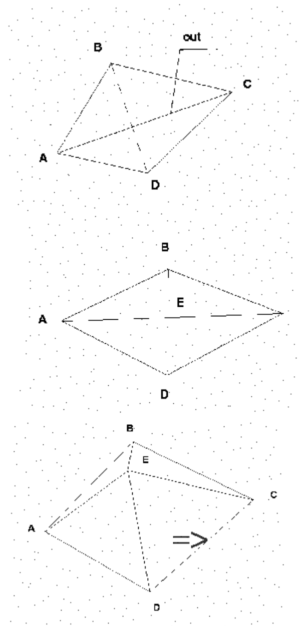

Elementary reconstruction: BD connection is introduced instead of AC connection. The total number of the knots and the cells in the grid is not changed.

Addition a knot at the middle of the connection: the knot E is added to the existing knots ABCD on the middle of the BD connection, 2 connections AE and EC appear and the total number of cells is increased by 2 cells.

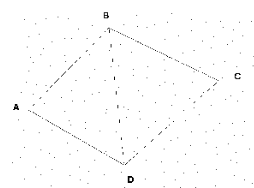

Removal a knot: the knot E is removed from the grid and the total number of the cells is decreased by 2 cells

Example of the triangular grid

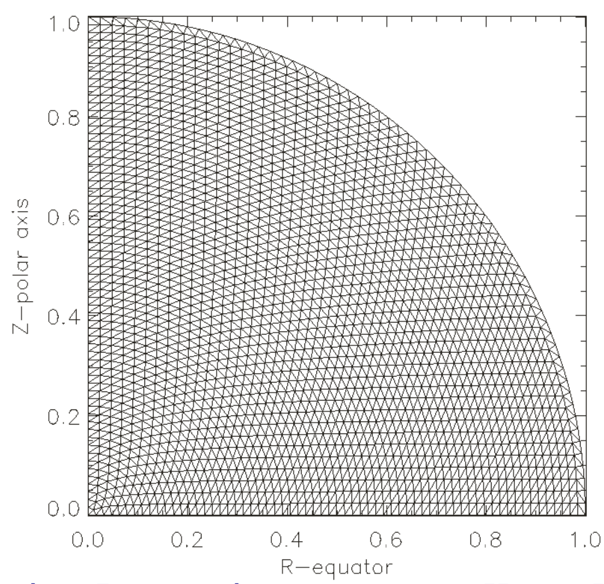

N.V.Ardeljan, G.S.Bisnovatyi-Kogan, K.V.Kosmachevskii, S.G.Moiseenko

1996, Astron. & Astrophys. Supl. Ser., **115**, 573

Collapse of a non-magnetized rotating protostellar cloud

Initial conditions: rigidly rotating uniform gas sphere

$$r = 3.81 \cdot 10^{16} cm, \rho = 1.492 \cdot 10^{-17} g/cm^3, M = 1.73 \cdot M_{\odot} = 3.457 \cdot 10^{33} g,$$

$$\gamma = \frac{5}{3}, u^r = u^z = 0, E_{rot0}/|E_{grav0}| = 0.04, E_{in}/|E_{grav0}| = 0.01,$$

Bounce and outburst.

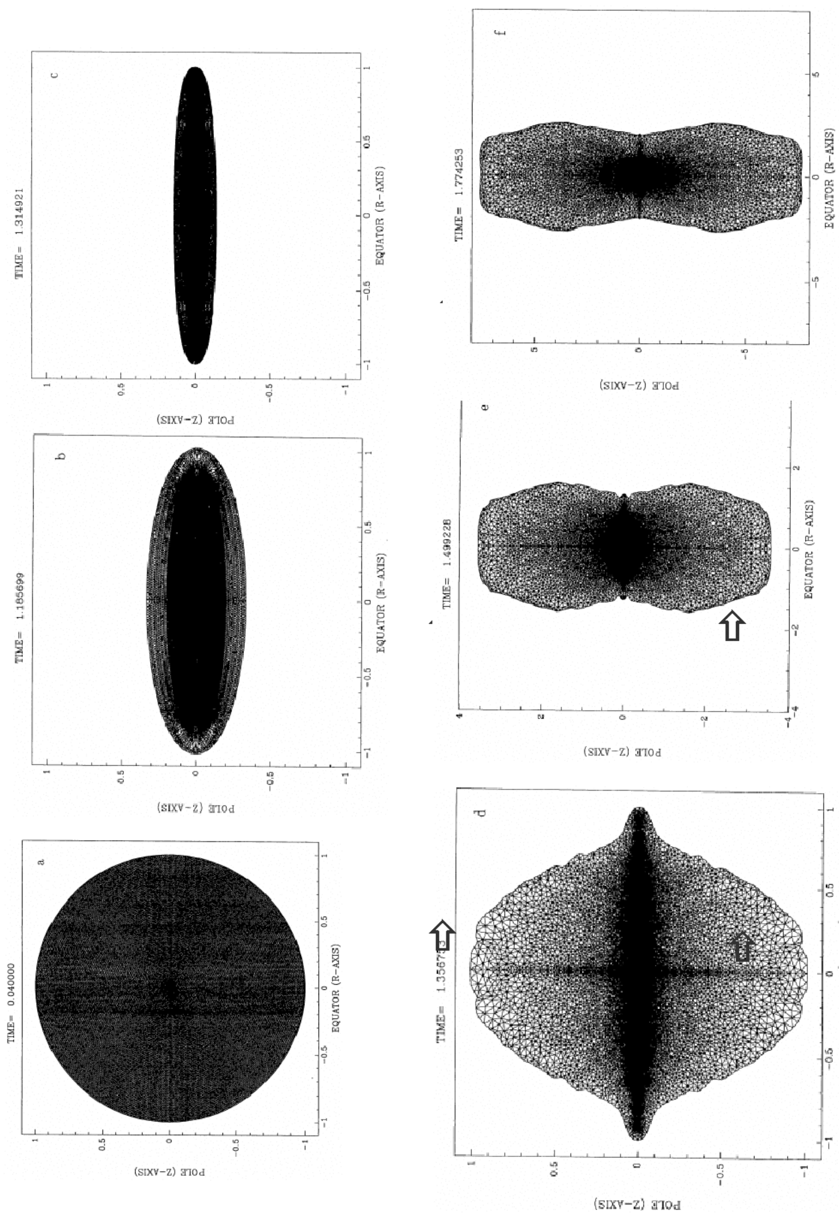

Grid reconstruction (example)

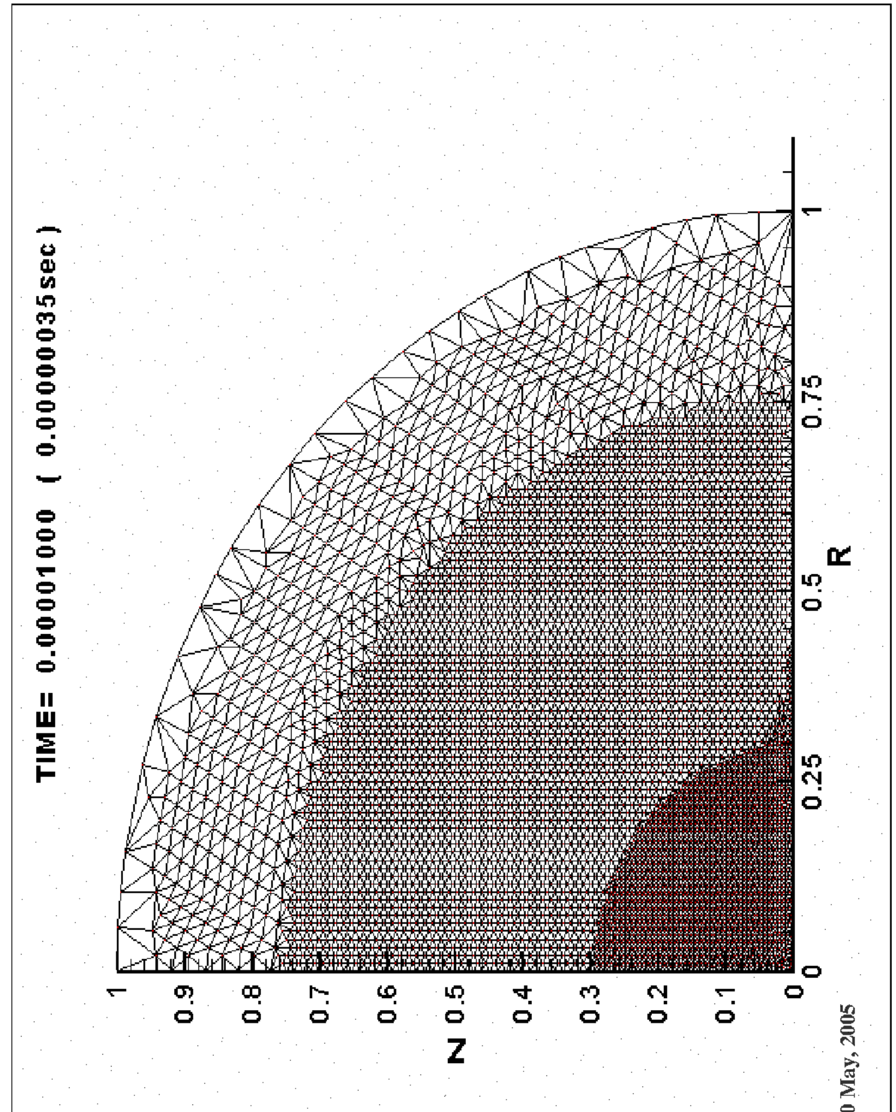

Grid reconstruction (example)

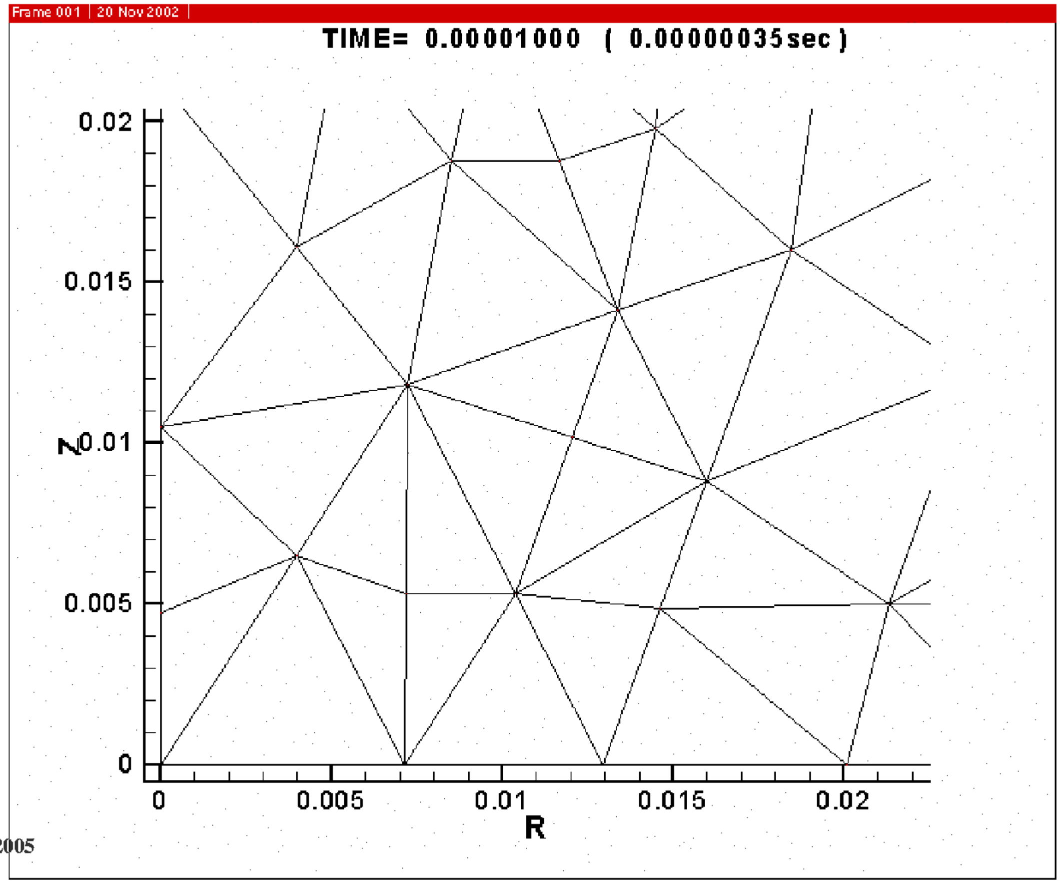

Presupernova Core Collapse

Ardeljan et. al., 2004, Astrophysics, **47,** 47

Equations of state takes into account degeneracy of electrons and neutrons, relativity for the electrons, nuclear transitions and nuclear interactions. Temperature effects were taken into account approximately by the addition of the pressure of radiation and of an ideal gas.

Neutrino losses and iron dissociation were taken into account in the energy equations.

A cool white dwarf was considered at the stability limit with a mass equal to the Chandrasekhar limit.

To obtain the collapse we increase the density at each point by 20% and switch on a uniform rotation.

Dr. Gennadi Bisnovatyi-Kogan, IKI (KITP Jets & Disks Program 5-20-05) Magnetorotational Supernovae Page 11

Gas dynamic equations with a self-gravitation, realistic equation of state, account of neutrino losses and iron dissociation

$$\frac{\mathrm{d}\mathbf{x}}{\mathrm{d}t} = \mathbf{v}, \quad \frac{\mathrm{d}\rho}{\mathrm{d}t} + \rho \nabla \cdot \mathbf{v} = 0,$$

$$\rho \frac{\mathrm{d}\mathbf{v}}{\mathrm{d}t} = -\nabla(P) - \rho \nabla \Phi,$$

$$\rho \frac{\mathrm{d}\varepsilon}{\mathrm{d}t} + P\nabla \cdot \mathbf{v} + \rho F(\rho, T) = 0,$$

$$\Delta \Phi = 4\pi G \rho.$$

$$P \equiv P(\rho, T) = P_0(\rho) + \rho \Re T + \frac{\sigma T^4}{3},$$

$$\varepsilon = \varepsilon_0(\rho) + \frac{3}{2}\Re T + \frac{\sigma T^4}{\rho} + \varepsilon_{Fe}(\rho, T).$$

ε_{Fe} -iron dissociation energy

F(ρ,T) - neutrino losses

KITP, 20 May, 2005

Equations of state (approximation of tables)

$$P \equiv P(\rho,T) = P_0(\rho) + \Re T\rho + \frac{T^4 \sigma}{3}$$

$$P_0(\rho) = \begin{cases} P_0^{(1)} = b_1 \rho^{5/3}(1 + c_1 \rho^{1/3}), for \rho \le \rho_1 \\ P_0^{(k)} = a \cdot 10^{b_k (\lg\rho - 8.419)^{c_k}} \; for \rho_{(k-1)} \le \rho \le \rho_k, k = \overline{2,6}. \end{cases} \quad \varepsilon_0(\rho) = \int_0^\rho \frac{P_0(x)}{x^2} dx.$$

$$\varepsilon = \varepsilon(\rho,T) = \varepsilon_0(\rho) + \frac{3}{2}\Re T + \frac{\sigma T^4}{\rho} + \varepsilon_{Fe}(\rho,T), \; \varepsilon_{Fe}(\rho,T) = \frac{E_{b,Fe}}{A_{m_p}}\left(\frac{T - T_{0,Fe}}{T_{1,Fe} - T_{0,Fe}}\right),$$

Fe –dis-sociation

Neutrino losses: URCA processes, pair annihilation, photo production of neutrino, plasma neutrino

URCA:

$$f(\rho,\overline{T}) = 1.3 \cdot 10^9 \chi(\overline{T}) / [1 + (7.1 \cdot 10^{-5} \rho / \overline{T}^3)^{2/5}] erg \cdot g^{-1} \cdot c^{-1}$$

$$\lambda(T) = \begin{cases} 1, \overline{T} < 7, \\ 664.31 + 51.024(\overline{T} - 20), 7 \le \overline{T} \le 20, \\ 664.31, \overline{T} > 20, \end{cases} \qquad \overline{T} = T \cdot 10^{-9}.$$

Approximation of tables from Ivanova, Imshennik, Nadyozhin,1969

$$F(\rho,T) = f(\rho,T) e^{-\tau_\nu}$$

KITP, 20 May, 2005

Initial State

Spherically Symmetric configuration, Uniform rotation with angular velocity 2.519 (1/сек). Temperature distribution: $T = \delta\rho^{2/3}$

$M = 1.0042 \cdot M_{sun}$ + 20%

Grid

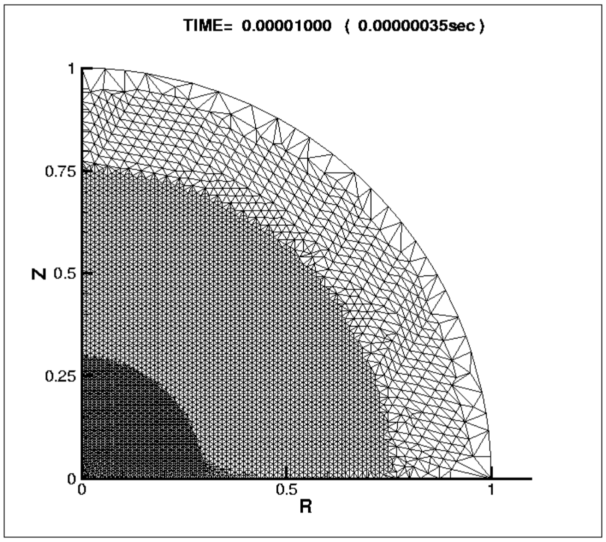

T

Density contours

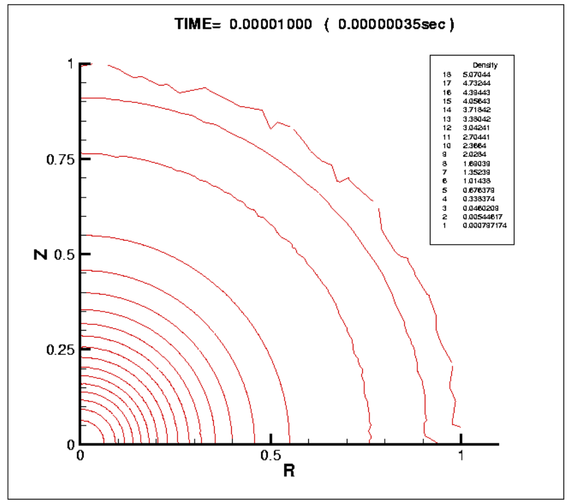

KITP, 20 May, 2005

Maximal compression state

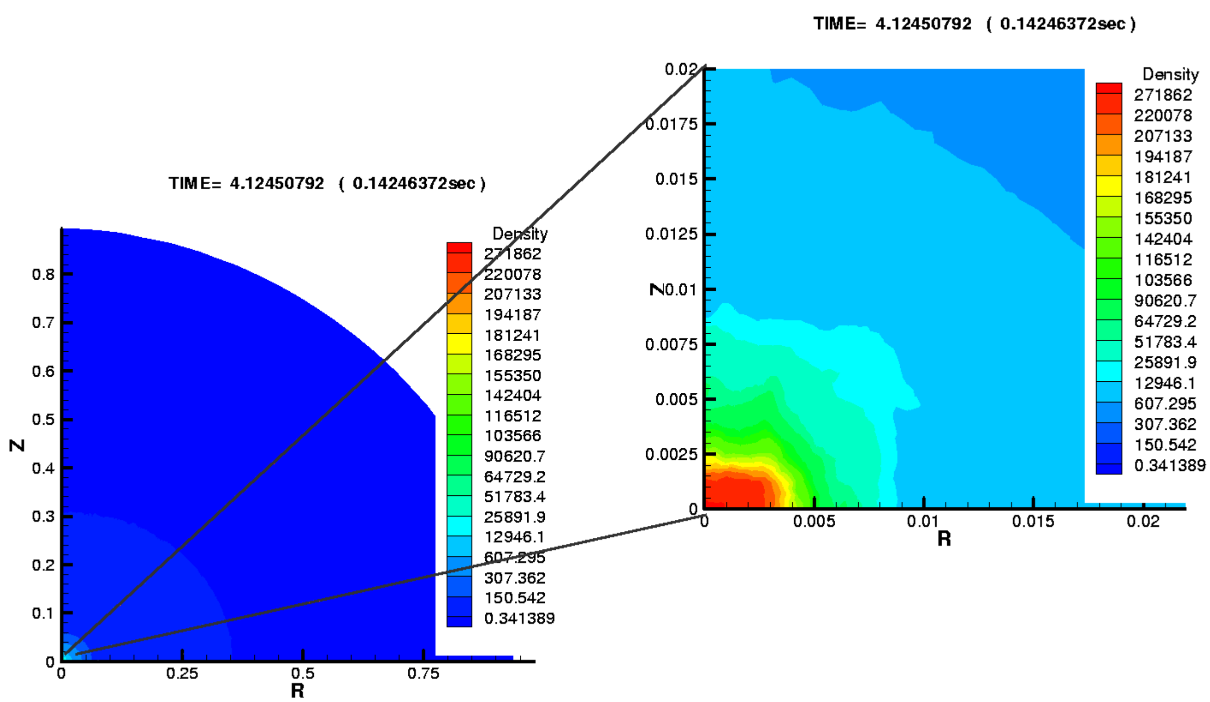

KITP, 20 May, 2005

Core formation and shock wave at its boundary

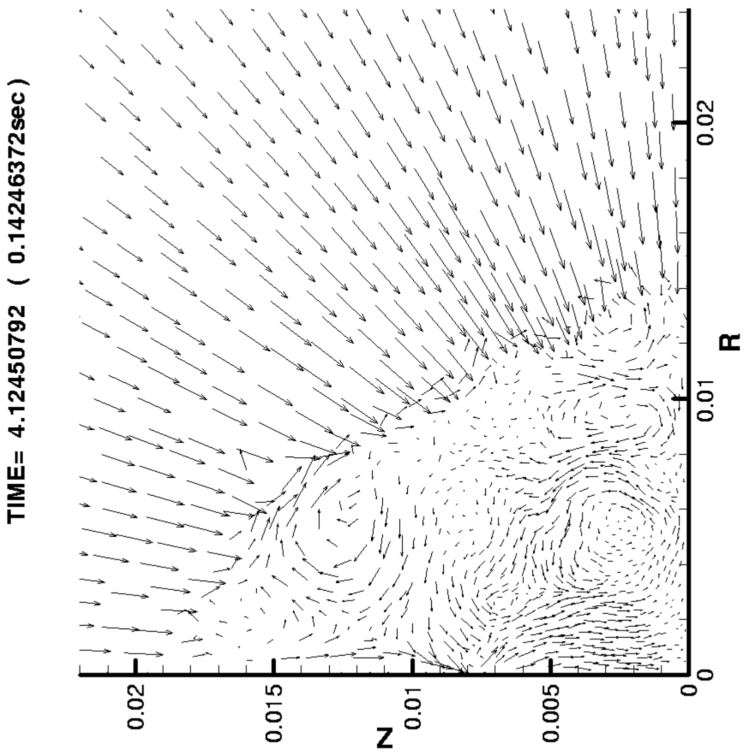

KITP, 20 May, 2005

Mixing

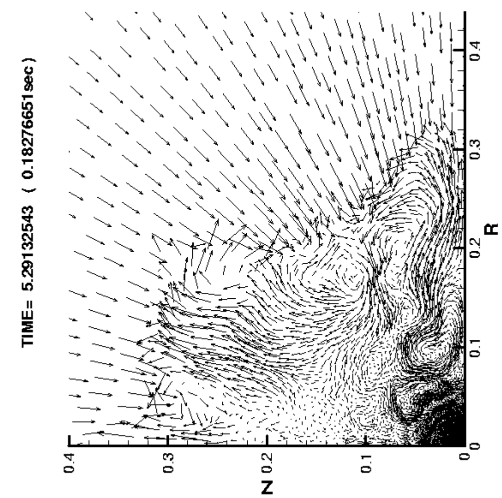

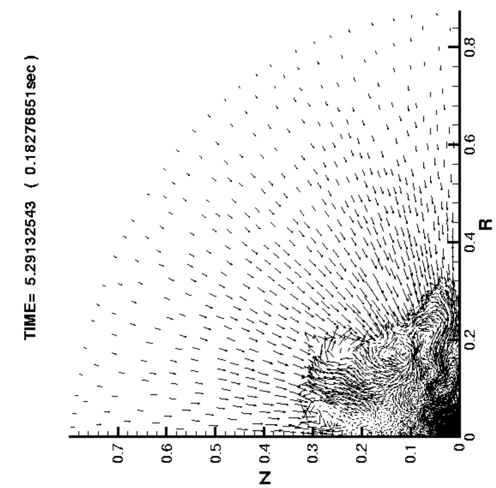

KITP, 20 May, 2005

Shock wave does not produce SN explosion :

Angular velocity (central part of the computational domain). Rotation is very differential.

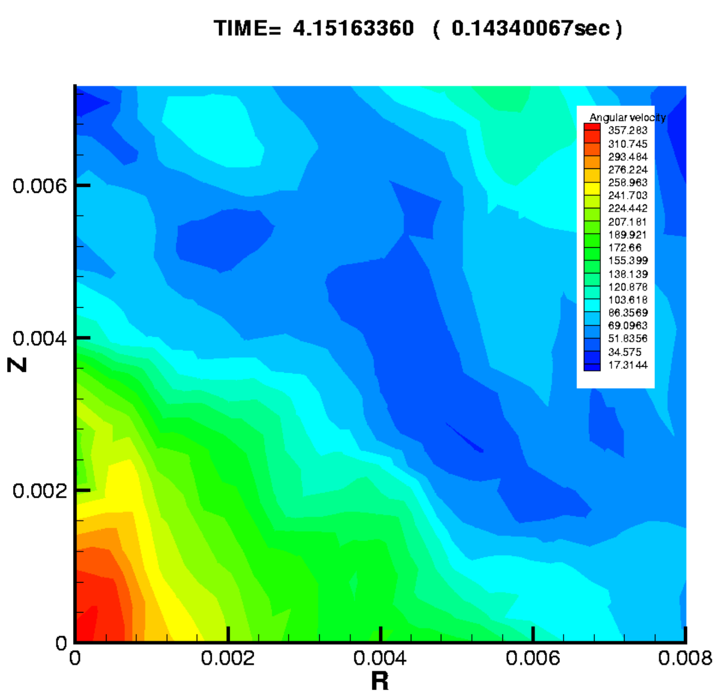

Distribution of the angular velocity

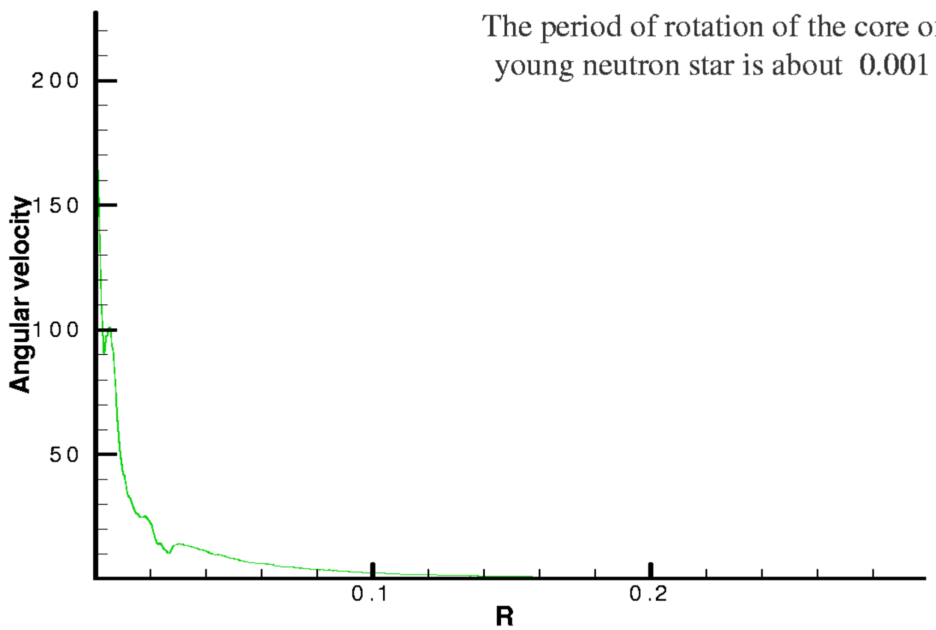

The period of rotation of the core of the young neutron star is about 0.001 sec

2-D magnetorotational supernova

N.V.Ardeljan, G.S.Bisnovatyi-Kogan, S.G.Moiseenko MNRAS, 2005, **359**, 333.

Equations: MHD + self-gravitation, infinite conductivity:

$$\begin{cases} \frac{dx}{dt} = \mathbf{u}, \frac{d\rho}{dt} + \rho \mathrm{div}\mathbf{u} = 0, \\ \rho \frac{du}{dt} = -\mathrm{grad}\left(p + \frac{\mathbf{H}\cdot\mathbf{H}}{8\pi} \right) + \frac{1}{4\pi}\mathrm{div}(\mathbf{H}\otimes\mathbf{H}) - \rho\,\mathrm{grad}\Phi \\ \rho \frac{d\varepsilon}{dt} + p\mathrm{div}\mathbf{u} + \rho F(\rho,T) = 0, p = P(\rho,T), \varepsilon = \mathrm{E}(\rho,T), \\ \Delta\Phi = 4\pi G\rho, \\ \rho \frac{d}{dt}\left(\frac{\mathbf{H}}{\rho}\right) = \mathbf{H}\cdot\nabla\mathbf{u}. \end{cases}$$

Additional condition: div**H**=0

Axial symmetry ($\frac{\partial}{\partial\phi} = 0$) , equatorial symmetry (z=0).

Boundary conditions

Rotational axis:

$$r = 0: u_r = u_\phi = H_r = H_\phi = \mathrm{rot}_r \mathbf{H} = \mathrm{rot}_\phi \mathbf{H} = 0,$$

Equatorial plane $u_z = H_z = 0,$ Quadrupole-like field

$z = 0:$ or

$$u_z = \frac{\partial B_z}{\partial z} = 0,$$ Dipole-like field

outer boundary : $P = \rho = T = H_\phi = 0, \mathbf{H}_{\mathrm{poloidal}} = \mathbf{H}_{\mathrm{q}}$

Initial toroidal current J_φ

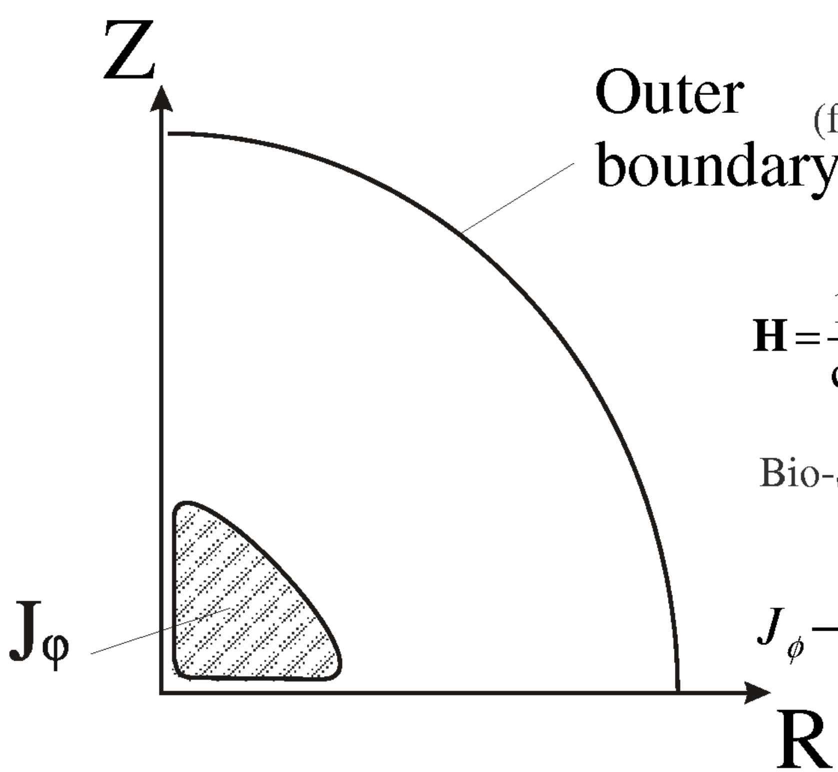

(free boundary)

$$\mathbf{H} = \frac{1}{c} \int \frac{\mathbf{J} \times \mathbf{R}}{R^3} dV,$$

Bio-Savara law

$$J_\phi -> (H_r, H_z)$$

Initial magnetic field –quadrupole-like symmetry

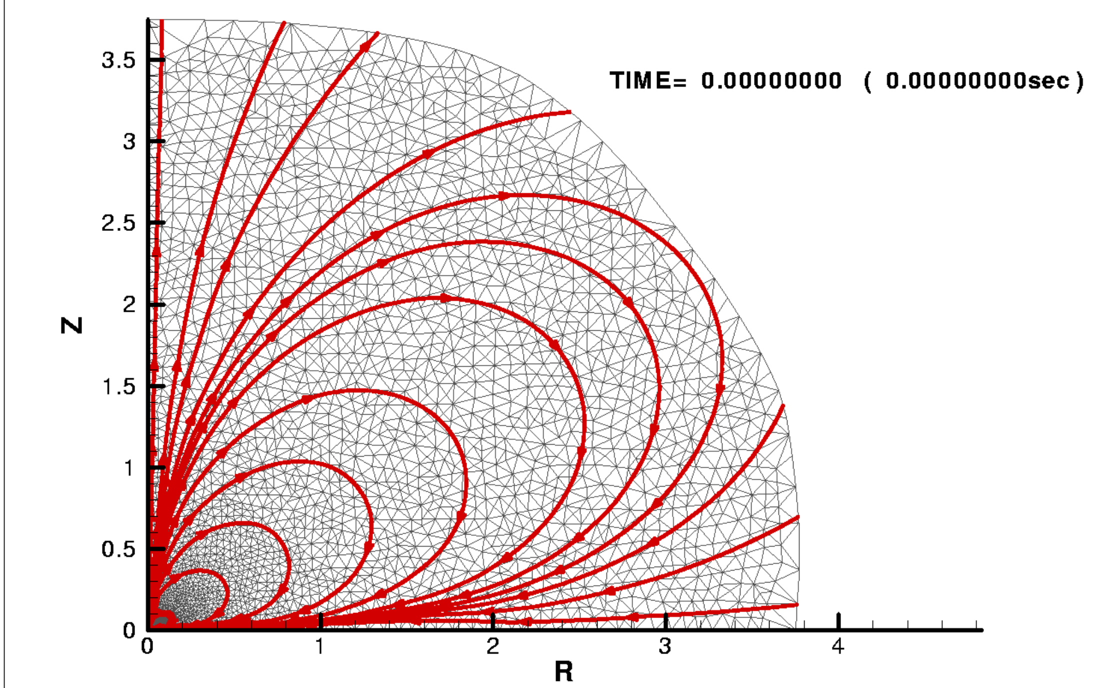

KITP, 20 May, 2005

Toroidal magnetic field amplification.

pink – maximum_1 of Hf^2 blue – maximum_2 of Hf^2

Maximal values of Hf=2.5 10(16)G

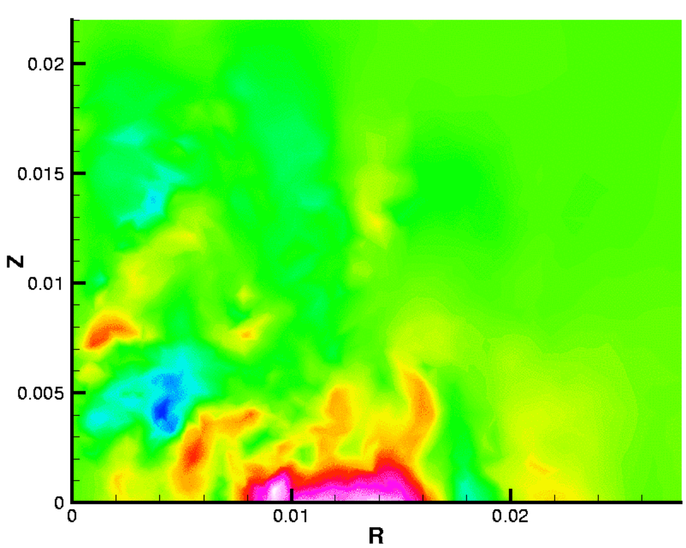

The magnetic field at the surface of the neutron star after the explosion is

$H = 4 \cdot 10^{12}$ Gs

KITP, 20 May, 2005

Temperature and velocity field

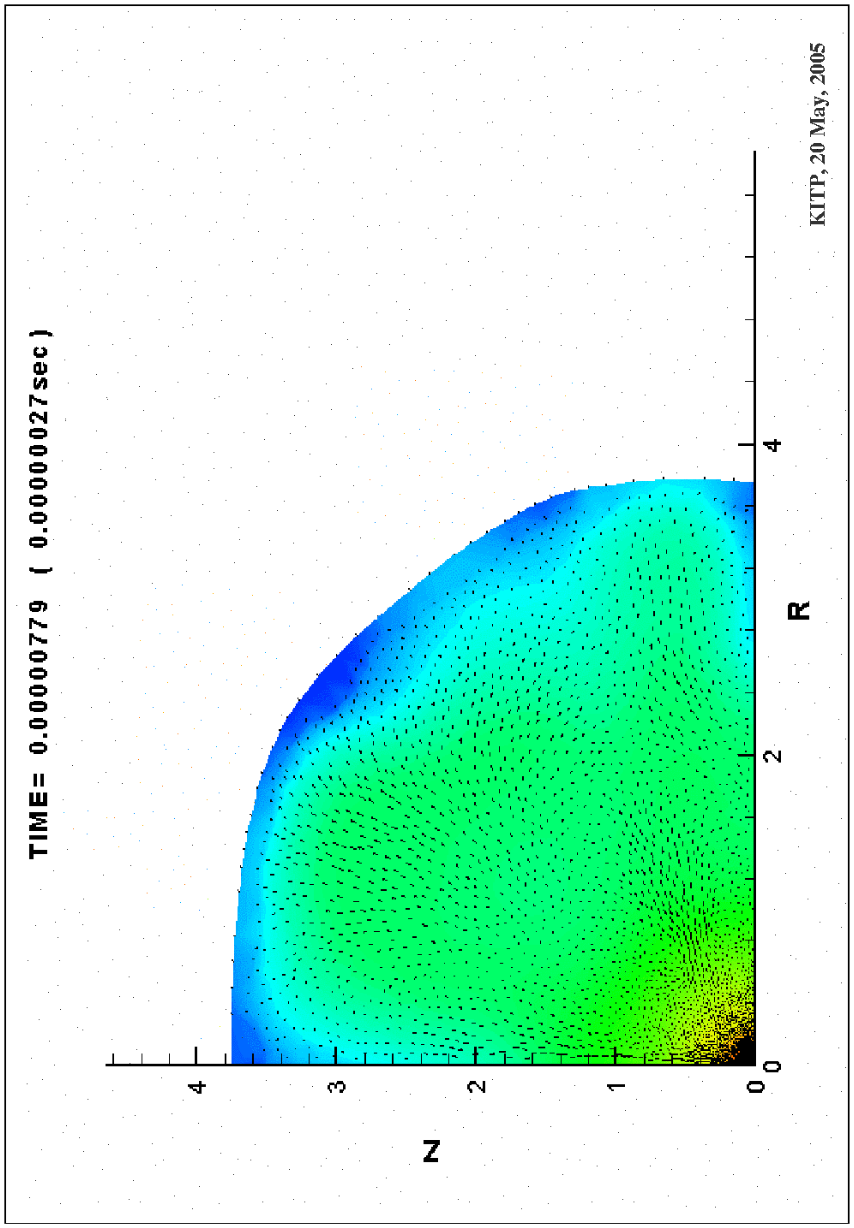

Specific angular momentum rV_φ

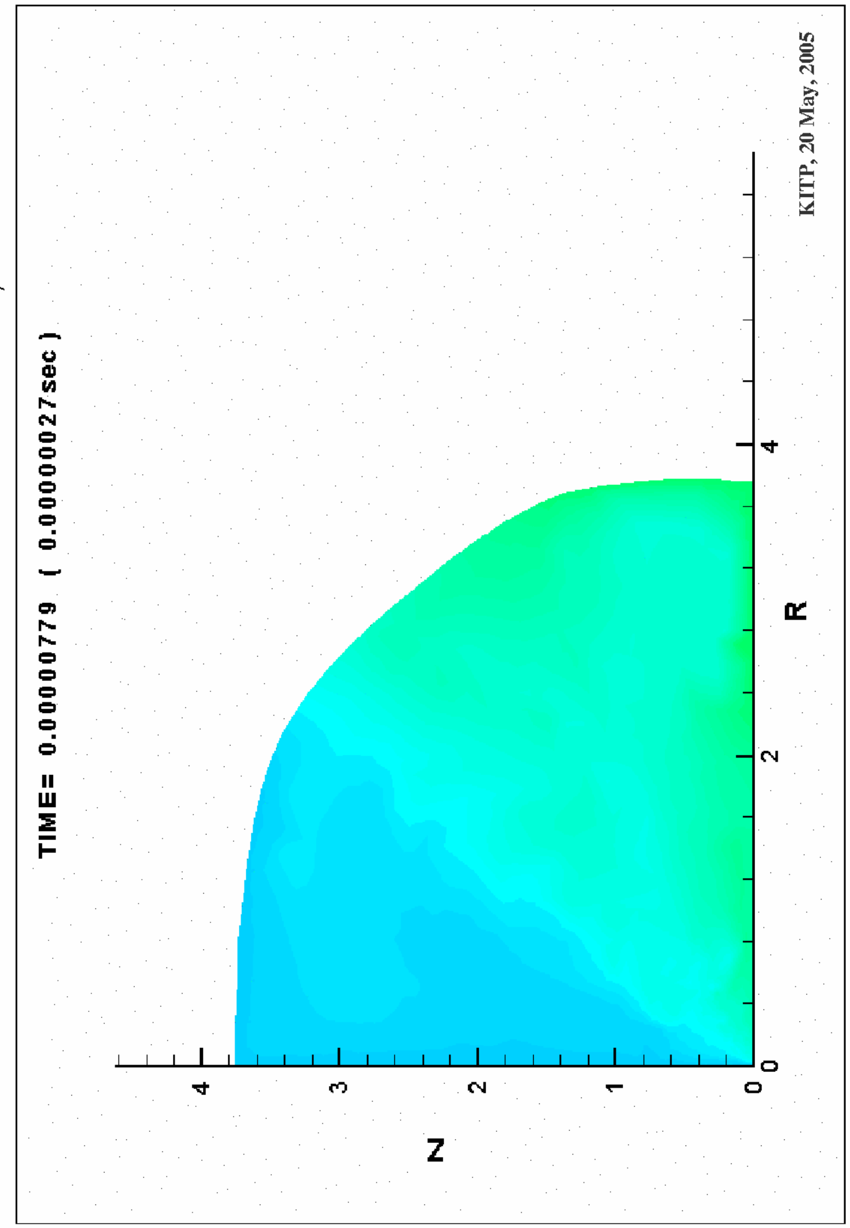

Time dependences

Rotational energy
Magnetic poloidal energy
Magnetic toroidal energy
Kinetic poloidal energy

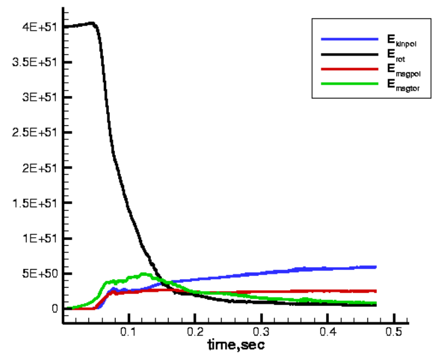

Gravitational energy

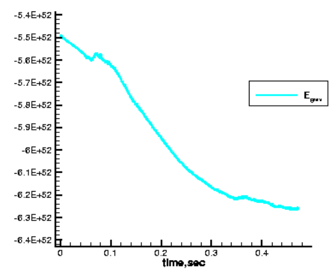

Internal energy

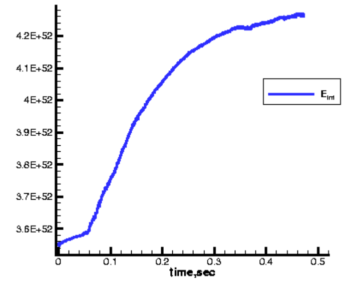

Neutrino losses

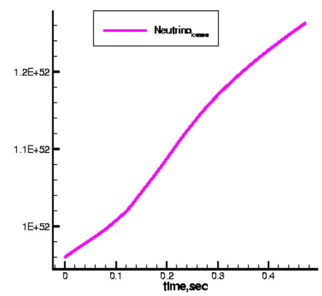

Neutrino luminosity

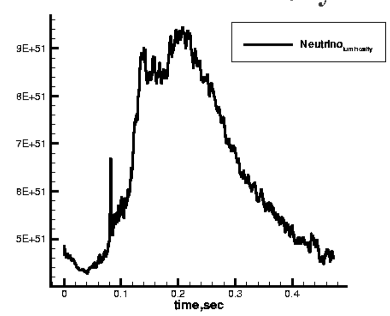

KITP, 20 May, 2005

Particle is considered "ejected" if its kinetic energy is greater than its potential energy

Ejected energy

0.6 10^{51} эрг

Ejected mass **0.14M$_{\odot}$**

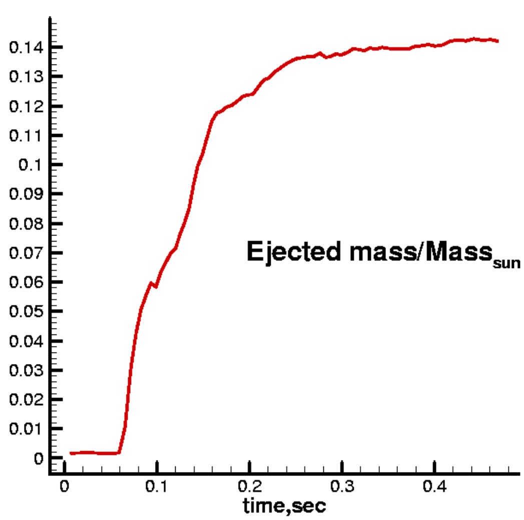

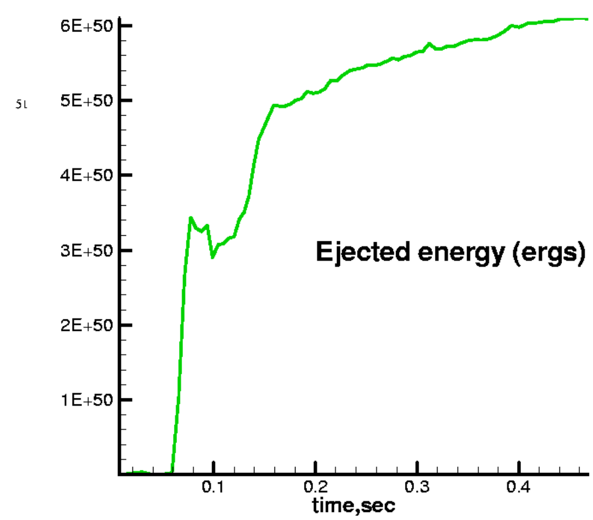

KITP, 20 May, 2005

Magnetorotational explosion at different $\alpha = 10^{-2} - 10^{-12}$

Magnetorotational instability ⇒ exponential growth of magnetic fields.
Different types of MRI:
Dungey 1958, Velikhov 1959, Balbus & Hawley 1991, Spruit 2002, Akiyama et al. 2003

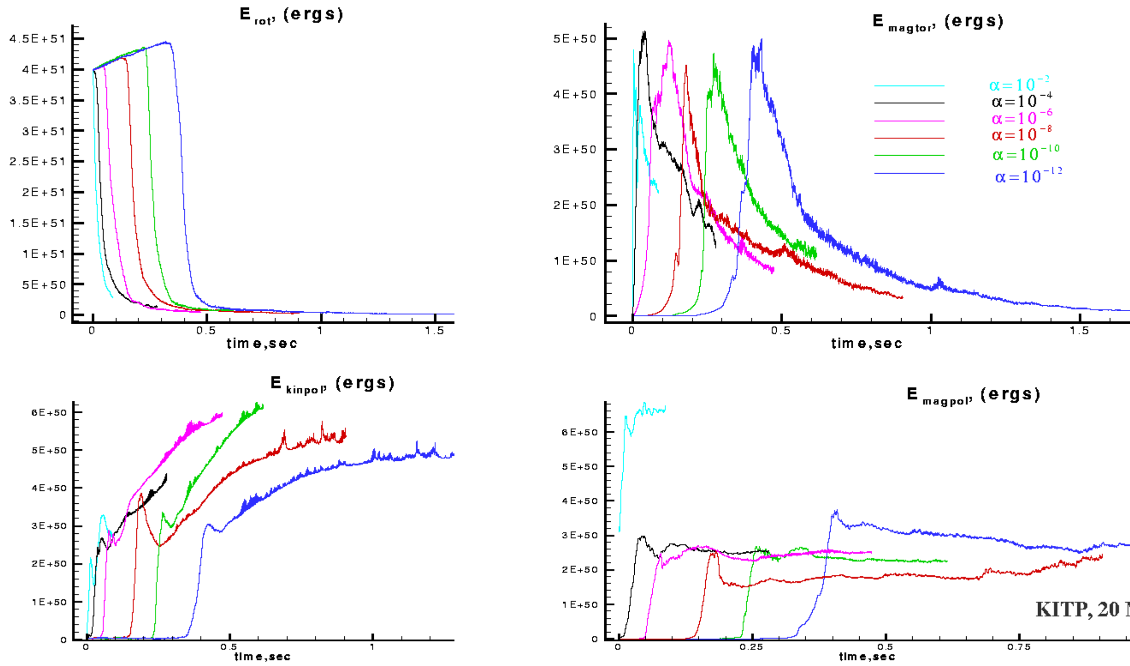

KITP, 20 May, 2005

Dependence of the explosion time on $\alpha = \frac{E_{mag0}}{E_{grav0}}$

1-D calculattions:
Explosion time

$$t_{взрыва} \sim \frac{1}{\sqrt{\alpha}}$$

$\alpha = 10^{-2} \Rightarrow t_{explosion} = 10,$
$\alpha = 10^{-12} \Rightarrow t_{explosion} = 10^{6}$ (!)

astro-ph/0410234

astro-ph/0410330

2-D calculattions:
Explosion time

$$t_{взрыва} \sim -\log(\alpha)$$

(for small α)

$\alpha = 10^{-6} \Rightarrow t_{explosion} \sim 6,$

$\alpha = 10^{-12} \Rightarrow t_{explosion} \sim 12.$

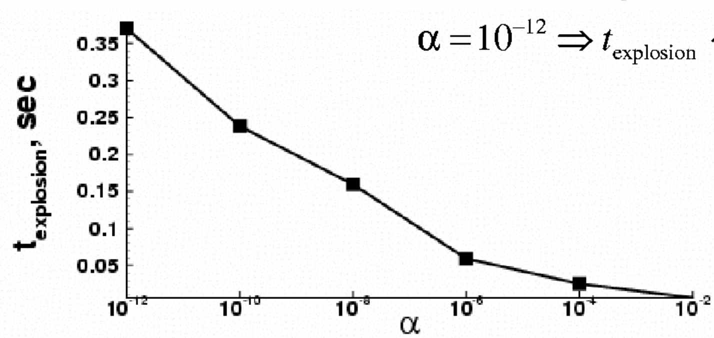

KITP, 20 May, 2005

Inner region: development of magnetorotational instability (MRI)

KITP, 20 May, 2005

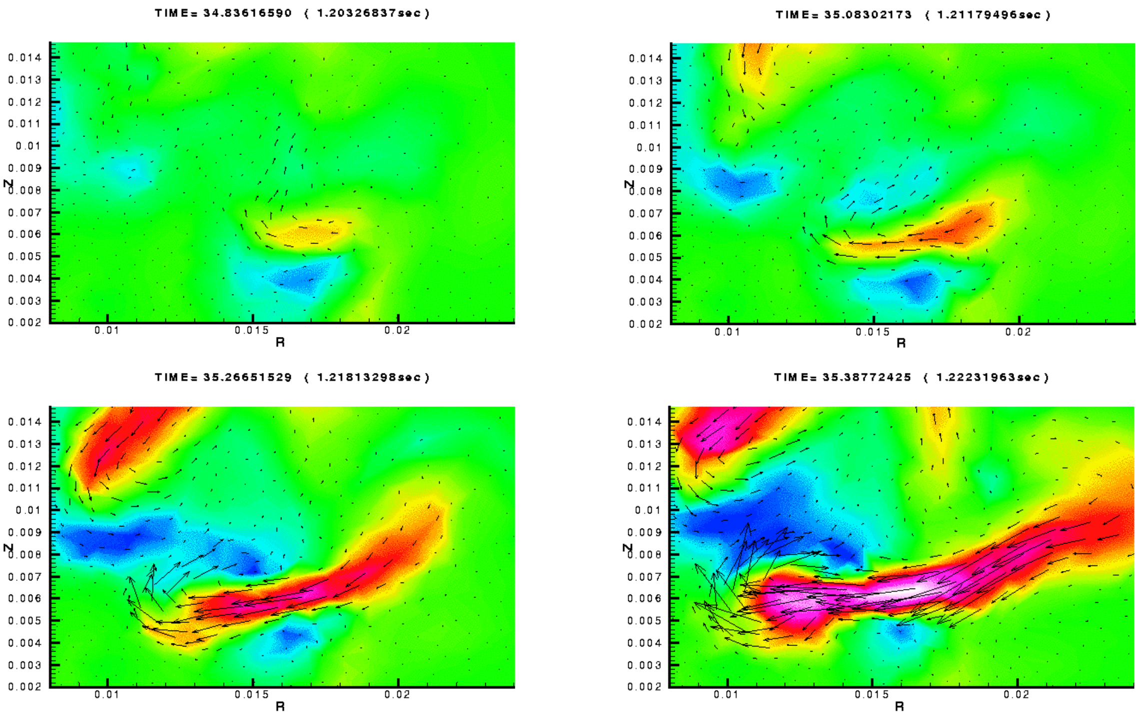

KITP, 20 May, 2005

Toy model of the MRI development: expomemtial growth of the magnetic fields

$$\frac{dH_\varphi}{dt} = H_r\left(r\frac{d\Omega}{dr}\right);$$ at initial stages $H_\varphi < H^*_\varphi$: $\left(r\frac{d\Omega}{dr}\right) = A \approx \text{const},$

MRI leads to formation of multiple *poloidal* differentially rotating vortexes. Angular velocity of vortexes is growing (linearly) with a growth of H_φ.

$$\frac{dH_r}{dt} = H_{r0}\left(\frac{d\omega_v}{dl}l\right), \qquad \left(\frac{d\omega_v}{dl}l\right) \approx \alpha(H_\varphi - H^*_\varphi).$$

$$\frac{d^2}{dt^2}\left(H_\varphi - H^*_\varphi\right) = AH_{r0}\alpha(H_\varphi - H^*_\varphi)$$

$$\Downarrow$$

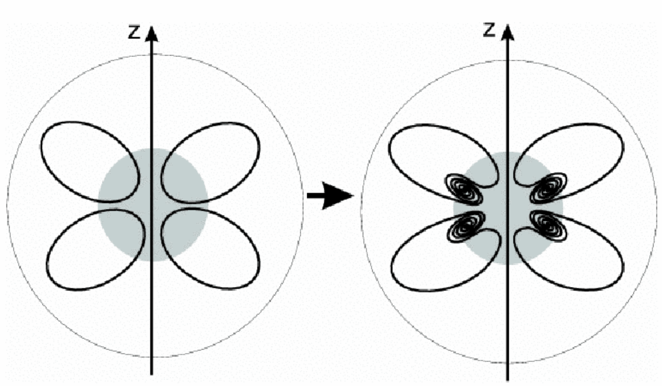

$$\begin{cases} H_\varphi = H^*_\varphi + H_{r0}e^{\sqrt{A\alpha H_{r0}}(t-t^*)}, \\ H_r = H_{r0} + \dfrac{H_{r0}^{3/2}\alpha^{1/2}}{\sqrt{A}}\left(e^{\sqrt{A\alpha H_{r0}}(t-t^*)} - 1\right). \end{cases}$$

KITP, 20 May, 2005

Jet formation in MRE

Dipole-like initial magnetic field

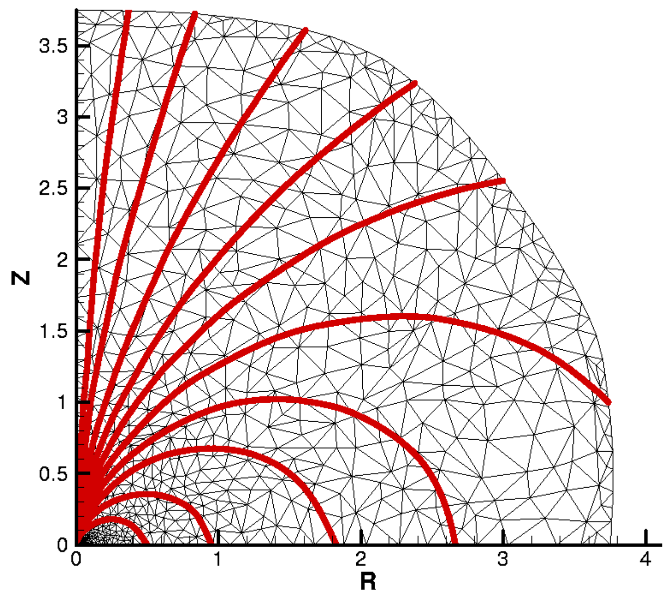

KITP, 20 May, 2005

Jet formation in MRE:

velocity field evolution

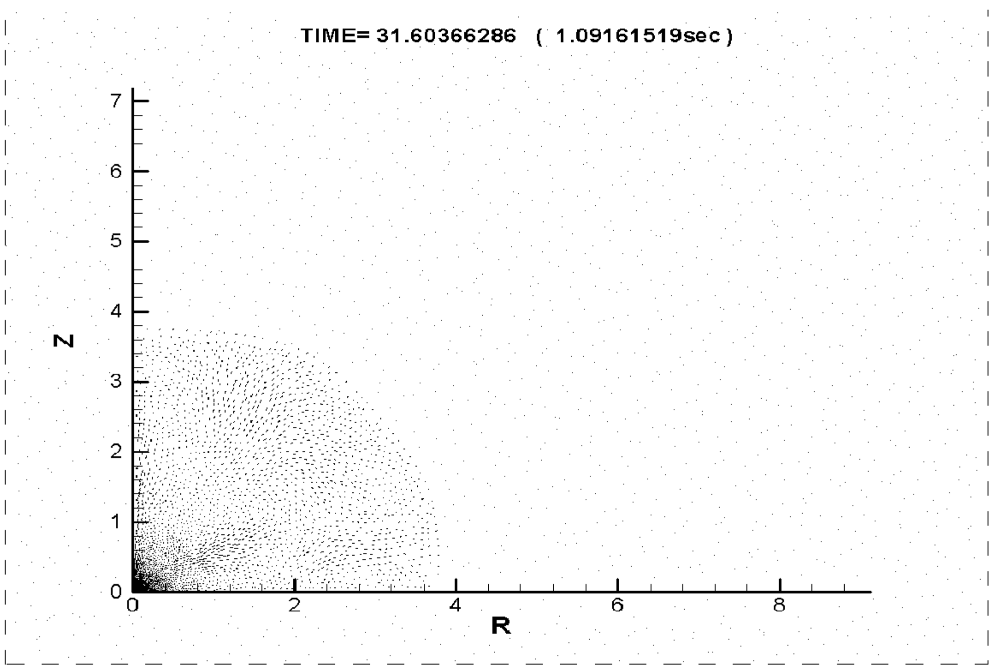

KITP, 20 May, 2005

Jet formation in MRE:

entropy evolution

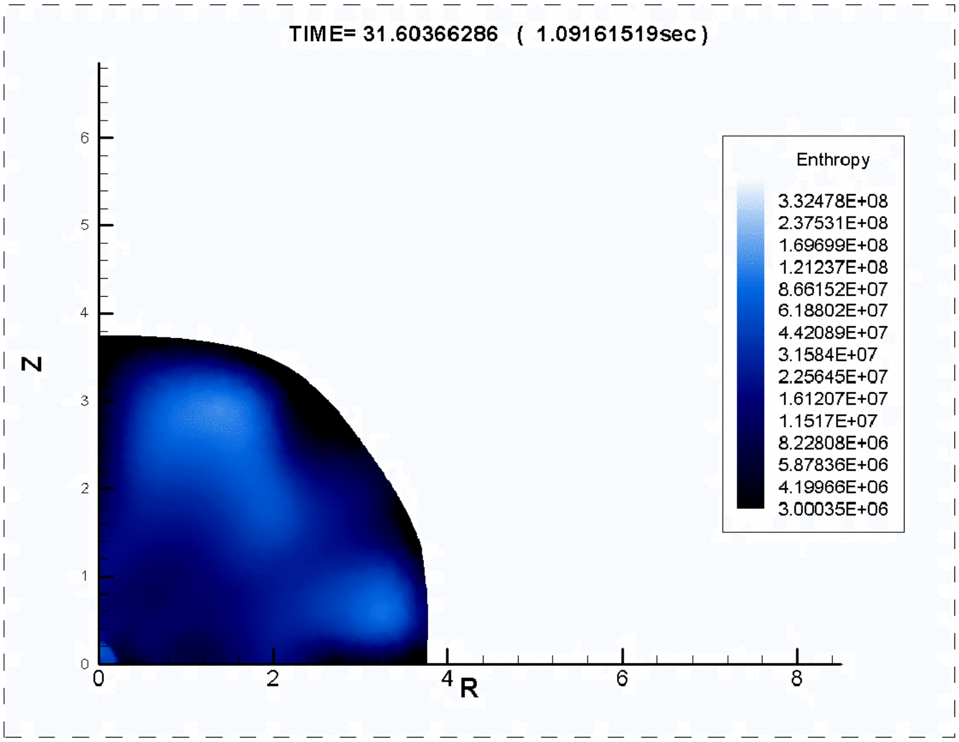

KITP, 20 May, 2005

Jet formation in MRE:

Angular momentum evolution

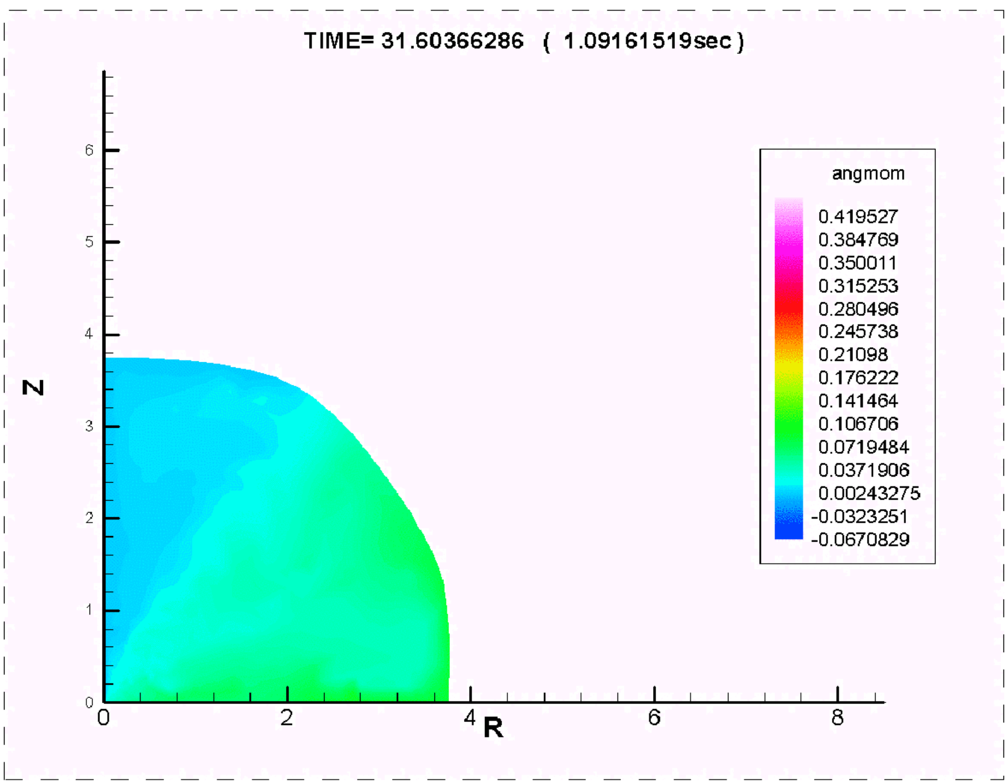

KITP, 20 May, 2005

Jet formation in MRE: (dipole magnetic field)

Energy of explosion≈$0.5 \cdot 10^{51}$эрг **Ejected mass ≈ $0.14 M_{\odot}$**

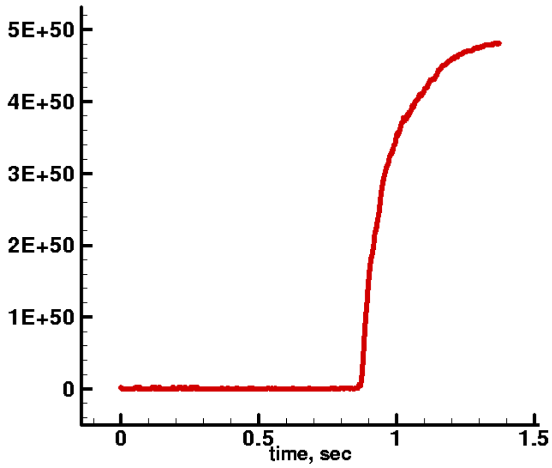

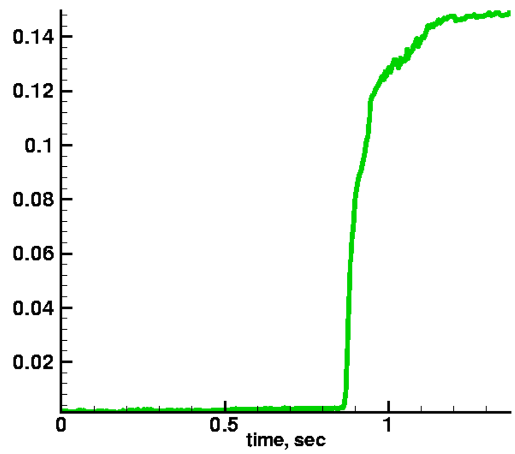

KITP, 20 May, 2005

Violation of mirror symmetry of magnetic field

(Bisnovatyi-Kogan, Moiseenko, 1992)

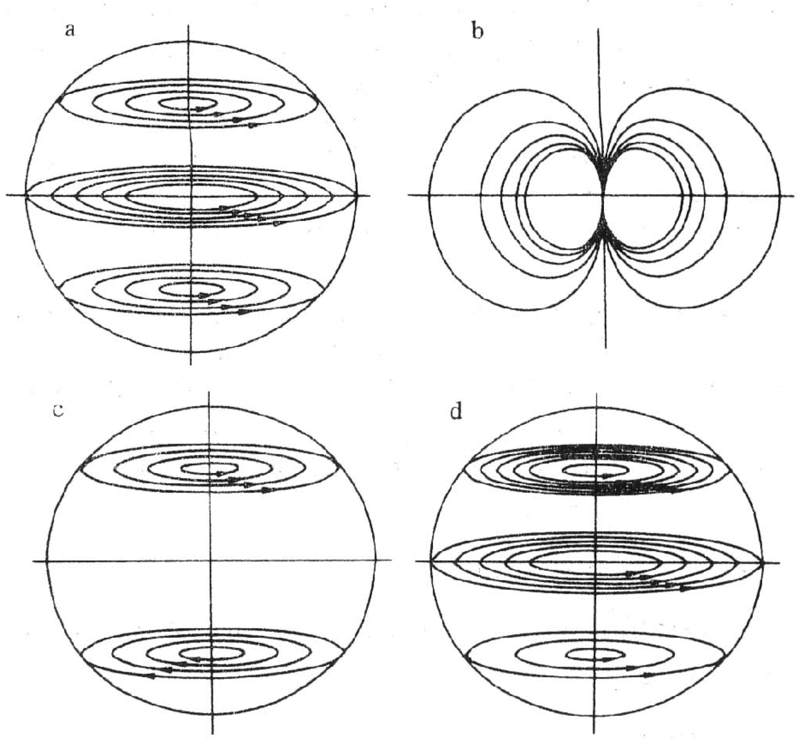

1. Initial toroidal field
2. Initial quadrupole field
3. Generated toroidal field
4. Resulted toroidal field

In reality we have dipole + quadrupole + other multipoles…

Lovelace et al. 1992

The magnetorotational explosion will be always asymmetrical.

Kick velocity due to the asymmetry of the magnetic field ~ up to 300km/sec

Bisnovatyi-Kogan, Moiseenko1992

Astron. Zh., **69**, 563

Interaction of the neutrino with asymmetric magnetic field – Kick velocity ~ up to 1000km/sec

Bisnovatyi-Kogan, 1993

Astron. Ap. Transactions **3,** 287

Conclusions

1. In the magnetorotational explosion (MTE) the efficiency of transformation of rotational energy into the energy of explosion is 10%. This is enough for producing core – collapse SN from rapidly rotating magnetized neutron star.
2. Development of magneto-rotational instability strongly accelerate MRE, at lower values of the initial magnetic fields.
3. The new born neutron star has inside a large (about 10^14 Gauss) chaotic magnetic field.
4. Jet formation is possible for dipole-like initial topology of the field: possible relation to cosmic gamma-ray bursts; equatorial ejection happens at prevailing of the quadrupole-like component.
5. Braking of the equatorial symmetry happenns in differentially rotating star with toroidal and poloidal components of an opposite symmetry; may explain formation of therapidly moving pulsars and one-side jet formation.